INNSPUB

Journal of Biodiversity and Environmental Sciences (JBES)
ISSN: 2220-6663 (Print) 2222-3045 (Online)
Vol. 20, No. 6, p. 81-90, 2022
http://www.innspub.net

RESEARCH PAPER OPEN ACCESS

Biogenic synthesis, characterization and antibacterial activity of Cu-Ag bimetallic nanoparticles using *Tabernaemontana divaricata*

E. Amutha[1], M. Esakki Raja[1], S. Rajaduraipandian[2], S. Gandhimathi[2], G. Annadurai[*1]

[1]*Sri Paramakalyani Centre of Excellence in Environmental Sciences, Manonmaniam Sundaranar University, Alwarkurichi, India*

[2]*Sri Paramakalyani College, Manonmaniam Sundaranar University, Alwarkurichi, India*

Article published on June 15, 2022

Key words: Green synthesis, Bimetallic nanoparticles, Antibacterial activity, Environmental remediation

Abstract

As such, green synthesis is regarded as an important tool to reduce the destructive effects associated with the traditional methods of synthesis for nanoparticles commonly utilized in laboratory and industry. They are environmentally friendly because the toxic chemicals produced during the biosynthesis of the nanoparticles can be degraded with the help of enzymes present in the microbes. In this work, we summarized the fundamental processes and mechanisms of green synthesis approaches, especially for bimetallic of Cu and Ag nanoparticles using natural extracts. The synthesized Cu-Ag nanoparticles were characterized by XRD, FT-IR, PSA, FL, and TGA. The antibacterial activity was tested on *B. subtilis, E. coli, Staphylococcus, Enterobacter* and *Pseudomonas*. The stability of nanoparticles and the associated surface engineering techniques for achieving biocompatibility are also discussed. Finally, we covered applications of such synthesized products to environmental remediation in terms of antimicrobial activity.

***Corresponding Author:** G. Annadurai ✉ gannadurai@msuniv.ac.in

Introduction

In materials science, "green" synthesis has gained extensive attention as a reliable, sustainable, and eco-friendly protocol for synthesizing a wide range of materials/nanomaterials including metal/metal oxides nanomaterials, hybrid materials, and bioinspired materials. Nanostructured metallic materials have been of great interest because the control of their size, distribution, structure, morphology and medium composition, allows absorbing and dispersing the energy of the medium in a different way compared to that in microscopic materials, changing drastically physical, chemical, mechanical, magnetic, biological, optical, electrical, physicochemical and catalytic properties (Liz-Marzan, 2004). In recent years, bimetallic NPs have been developed and used for various applications in the fields of chemistry, material science, biotechnology, and environmental protection. Bimetallic NPs containing copper (Cu) and silver (Ag) with a high fraction of surface atoms and high specific surface area have been widely studied (Ikram *et al.,* 2020). Therefore, many studies are required to develop simple shape-controlled synthesis methods of Ag/Cu bimetallic nanoparticles (Ag/Cu NPs) (Li *et al.,* 2015*;* Liu *et al.,* 2014). Silver nanoparticles synthesis using the plant. Leaf extract mediated silver nanoparticles synthesis of *Capparis spinosa* L. was evaluated for biological activity (Cioffi *et al.,* 2005). The antimicrobial properties of silver NPs are well-established with several mechanisms for their bactericidal effects being proposed (Chaloupka *et al.,* 2010; Xiu *et al.,* 2012; Pal *et al.,* 2009; Sondi and Salopek-Sondi, 2004), copper NPs have also been shown to act promisingly as bactericidal agents, although only a few studies on their antibacterial properties have been reported (Jeon *et al.,* 2003). Many researchers examine that Cu NPs being less expensive as compared to Ag NPs and display improved antibacterial and antimicrobial activities (Dang *et al.,* 2011; Liu *et al.,* 2015; Sun and Xia, 2002). Beside this, the synthesis of Cu NPs is more challenging than that of Ag nanoparticles, because Cu NPs get oxidized very quickly during synthesis and lead to the formation of secondary compounds such as CuO, Cu_2O and $Cu(OH)_2$ than that of mono atomic Cu metal (Tan *et al.,* 2013; Tan *et al.,* 2010*; (Ma et al.,* 2016*).* In this paper we report preparation of Cu-Ag bimetallic nanoparticles in environmentally benign stabilizing agent via a green route and the antibacterial activity of both the as such stabilized metal solutions. The antimicrobial properties of Cu-Ag bimetallic nanoparticles are well-established and several mechanisms for their bactericidal effects have been proposed. Although only a few studies have reported the antibacterial properties of Cu-Ag bimetallic nanoparticles, they show Cu-Ag bimetallic nanoparticles have a significant promise as bactericidal agent.

Materials and methods

Chemicals and Plant Material Collection

All the reagents purchased were of analytical grade and used without any further purification. Silver nitrate ($AgNO_3$) and Copper nitrate ($CuNO_3$) was purchased from Sigma-Aldrich with ≥ 99.5% purity. Fresh leaves of *Tabernaemontana divaricata* was collected from the local area land, Idaikal, India. Distilled water was used for preparing aqueous solutions all over the experiments.

Preparation of Leaf Extract

Fresh leaves of *Tabernaemontana divaricata* were collected and washed with tap water at first, and then the surface was washed under running water with distilled water until no impurities remained. Then, the fresh leaves were cut and weighed about 10g and dissolved in 100mL of distilled water. The mixture was heated for 20 minutes at 60°C while stirring occasionally and then allowed to cool at room temperature (Marslin *et al*., 2018). The mixture was filtered using the Whatman no:1 filter paper. The extract was stored in the refrigerator for further use to synthesize Ag nanoparticles from the $AgNO_3$ precursor solution.

Green Synthesis of Cu-Ag Bimetallic Nanoparticles

$AgNO_3$ powder was dissolved in distilled water to prepare a 200mL stock solution in a flask and maintained in magnetic stirrer for 20 minutes. $CuNO_3$

powder was dissolved in distilled water to prepare a 200mL stock solution in a flask and maintained in magnetic stirrer for 20 minutes. Both the metal salt solutions were mixed and heated for 10 min at 95°C. 40mL of the plant extract was added to the salt solution. The mixture was maintained at room temperature for 24 h followed by centrifugation, and dried at Hot air over at 60°C for 24 h.

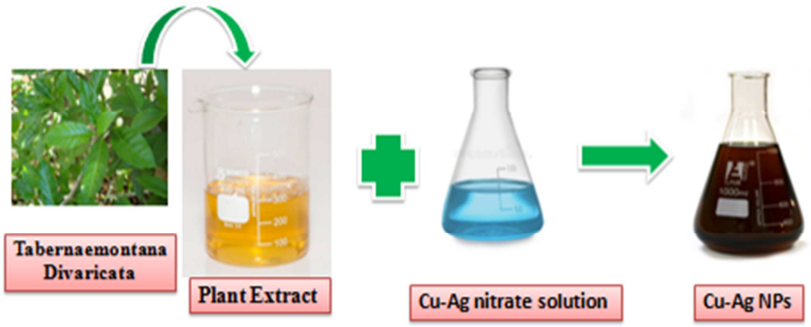

Fig. 1. Synthesis of Cu-Ag NPs.

Antibacterial activity of bimetallic NPs

Agar Well Diffusion Assay

The antibacterial property of the Cu-Ag NPs was determined by using the bacterial species including the pathogenic bacteria such as Gram-positive *Staphylococcus aureus* and *Bacillus subtilus*, and Gram-negative *Escherichia coli*, *Enterobacter,* and *Pseudomonas fluorescens* by the well diffusion method. The different concentrations used were at 25µl, 50µl, 75µl and 100µl for the identification of antimicrobial activity of the above bacterial species. All the plates were incubated at 37°C for 24 hours, and the zone of inhibition of bacteria was measured.

Result & discussion

UV Visible Spectroscopy Analysis

The UV-vis spectra were measured to characterize optical properties of Ag-Cu NPs (Fig. 2). The absorption spectrum of Ag-Cu NPs gives a typical surface plasmon resonance (SPR) band of Ag from 210 to 350nm with a peak at about 245nm. The synthesized silver and copper nanoparticles covered with biomolecules are well dispersed in solutions and fairly stable up to 3 months as indicated by retention of brown Colour of the solution. In case of copper nanoparticles, these results clearly indicate the formation of mixture of CuO and Cu_2O nanoparticles as previously reported in literature [Yin *et al.*, 2005, Rahman *et al.*, 2009].

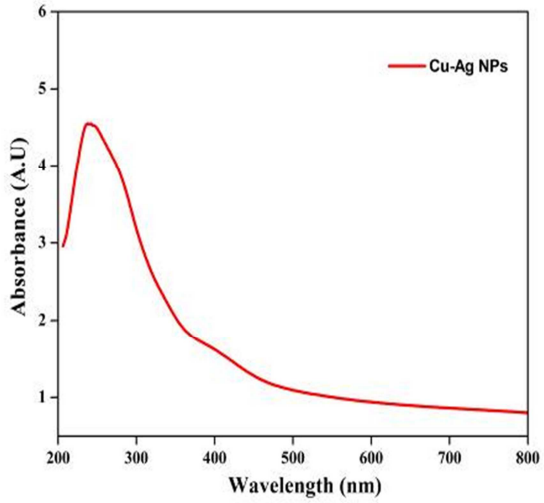

Fig. 2. UV spectrum of Cu-Ag NPs.

Fourier Transform Infrared Spectroscopy Analysis

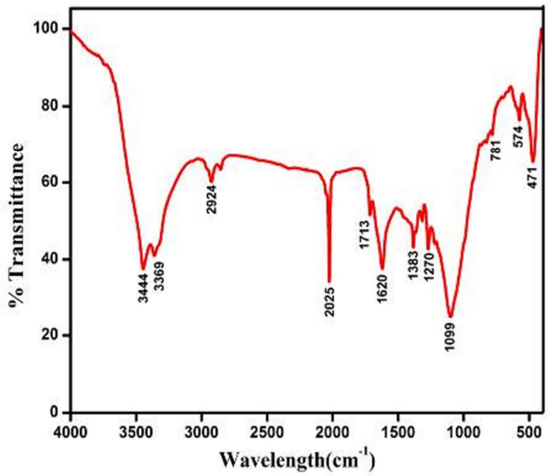

Fig. 3. FT-IR spectra of Cu-Ag NPs.

FTIR analysis has been done in the wave number range from 450/cm to 4000/cm. The sample was admixed with KBr, thoroughly mixed and pelletized by pressing under sufficient pressure before FTIR analysis. Cu-Ag NPs are analysed by FTIR spectrometer and are shown in Fig. 3. The peak for O-H stretch, H-bonded alcohols, phenols was obtained at 3444cm^{-1} . The peaks at 3369 and 2924cm^{-1} are associated with N-H stretch1°, 2° amines, amides and C-H stretch alkanes (Therese Marie and Drexel, 2016; Hikmah *et al.*, 2016). The peak at 2025cm^{-1} is associated with Nitrile C≡N Stretch. The peak at 1713cm^{-1} indicated C=O (saturated aldehyde) Aldehydes & Ketones and that at 1620cm^{-1} was associated with C=C stretch (conjugated) alkenes. The peak for the carbonyl group was obtained at 1383cm-1. The peaks at 1270 and 1099cm^{-1} are associated with C—O carboxylic acids and C-N Amines. The peak for C-Br stretch alkyl halides was obtained at 574cm^{-1}. The peaks indicated the existence of many functional groups in the aqueous extract of *Tabernaemontana divaricata* liable for the formation of stable Cu-Ag NPs (Therese Marie and Drexel, 2016; Hikmah *et al.*, 2016).

Table 1. Peak table of Cu-Ag NPs.

SN	Peak (cm^{-1})	Functional Group
1	3444	O-H stretch, H-bonded alcohols, phenols
2	3369	N-H stretch1°, 2° amines, amides
3	2924	C-H stretch alkanes
4	2025	Nitrile C≡N Stretch
5	1713	C=O (saturated aldehyde) Aldehydes & Ketones
6	1620	C=C stretch (conjugated) alkenes
7	1383	C-F stretch alkyl halides
8	1270	C—O carboxylic acids
9	1099	C-N Amines
10	781	C-H bend (mono) aromatics
11	574	C-Br stretch alkyl halides

X-ray diffraction analysis

The phase and crystal structure of the synthesized nanoparticles are studied using XRD analysis. XRD patterns of Ag-Cu nanoparticles are shown in Fig. 4. The main characteristic diffraction peaks for silver are observed 27.6, 46.06, 54.65, 67.30 and 77.19 with correspond to crystallographic planes of (110), (111), (211), (222) and (311) respectively (Klabunde and Richards, 2001;). There are three main characteristic diffraction peaks for copper observed 32.0 and 74.29 with correspond to crystallographic planes of (111) and (220). The results are similar to the results as reported by Jawhara *et al.*, (2019) where all eight characteristic diffraction peaks of silver and copper appeared (Niu *et al.*, 2018).

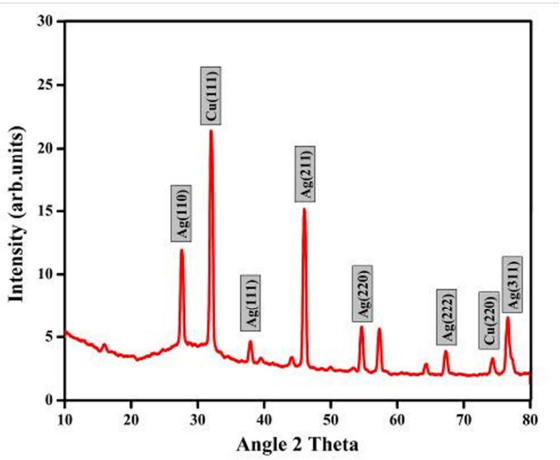

Fig. 4. XRD pattern of Cu-Ag NPs.

All the peaks are well indexed to face centered cubic (fcc) phase of crystalline Ag (JCPDS card no.4-783) and fcc phase of crystalline Cu (JCPDS card no. 4-836). The peaks corresponding to bimetallic NPs fall in between the peaks of Ag and Cu indicating that the new phases formed are homogenous Ag-Cu alloy phases rather than completely separated phases of Ag and Cu. The difference in lattice parameter also indicates the formation of alloy NPs (Valodkar *et al.*, 2011; Sonal *et al.*, 2019). The silver nanoparticles contain high atomic density facet as (111) in all samples that are known to be highly reactive (Hikmah *et al.*,2016). The average crystalline size of Cu-Ag bimetallic nanoparticle is 24nm.

Scanning electron microscopy analysis

The SEM images justify the structural and morphological behavior of the bimetallic nanoparticles. From SEM analysis (Fig. 5), it was observed that the three different morphologies of Cu-Ag bimetallic samples are successfully obtained, including cube, rod and trapezium nanostructures (Tamayo *et al.*, 2014; Li *et al.*, 2015). It is also analyzed that with the increase of Cu molar ratio, surface area becomes high because, with the

impregnation of nanoparticles, micropores get developed on biosynthesis.

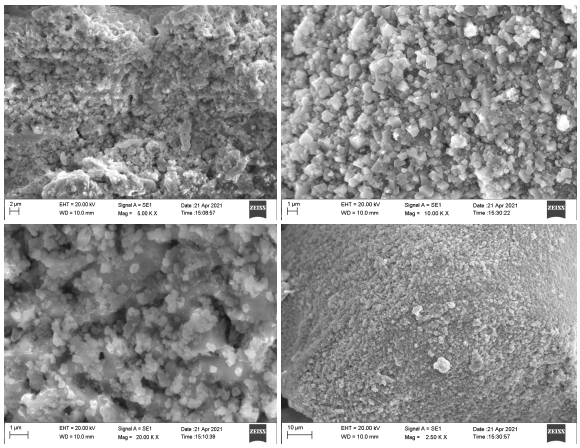

Fig. 5. SEM micrographs of Cu-Ag NPs.

Further, EDS with elemental mapping was used to confirm the bimetallic structure and the distribution of Ag/Cu (Manisha Sharma *et al., 2017*). The mean grain size of bimetallic Ag-Cu NPs was found to be ~ 100nm. Likewise, (Shankar *et al.* 2003; Deepika Sharma *et al.*, 2020) have also reported the average crystallite size between the ranges of 80-120nm for Ag-Cu NPs.

EDX analysis was carried out to understand the semi quantitative elemental composition of copper and silver particles. The peaks showed the presence of copper and silver (Fig. 6) particles (Liu *et al.,* 2014). Total metal content was quite high to justify the purity of metallic nanoparticles.

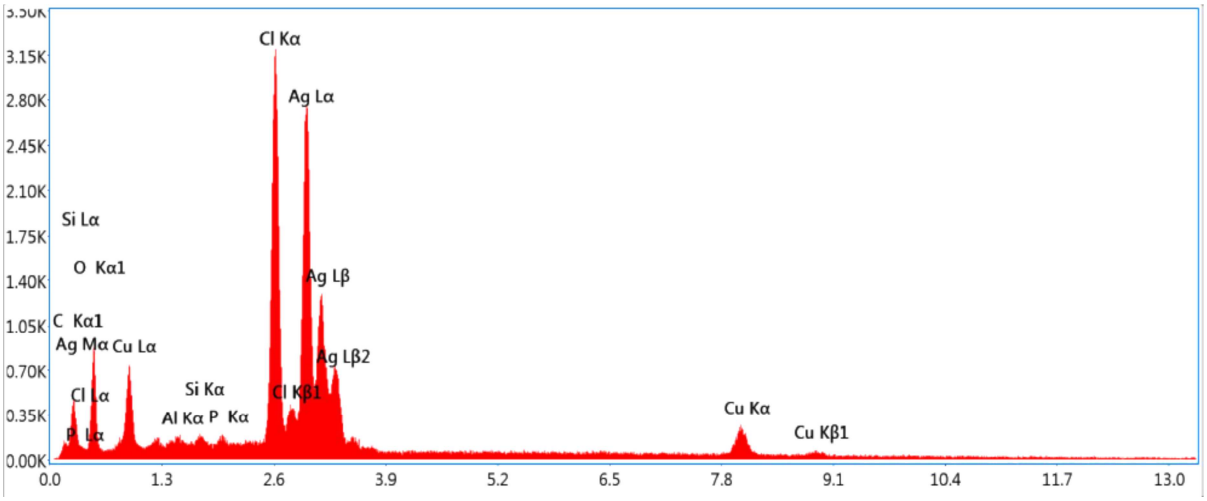

Fig. 6. EDS Spectrum of Cu-Ag NPs.

Dynamic Light Scattering analysis

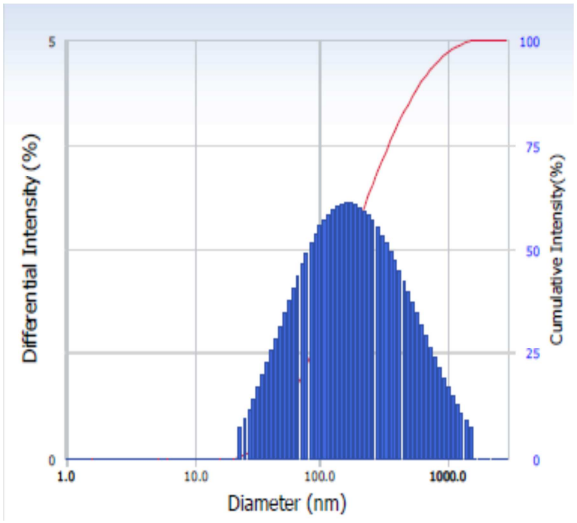

Fig. 7. DLS image of Cu-Ag NPs.

The synthesized Cu-Ag NPs were ultra sonicated and suspended in the ethanol solution. The sizes of the agglomerated colloids in the suspensions were estimated using particle size analyzer (PSA). From the analysis the particle size is found to be 60nm and is in good accordance with the crystallite size of Cu-Ag NPs i.e. twice that of the crystallite size (Chattopadhyay and Patel 2009). The particle size distribution and average particle Size of Cu-Ag NPs results are shown in Fig. 7. The formation of physical mixture in both samples however, can be ruled out since the bimetallic nanoparticles are different in a lot of aspects such as dispersion color, surface plasmon resonance (UV), shape or morphology (SEM), among others.

The distribution of each metal within a particle and their organization is known to vary depending on the synthetic approach used in the preparation of bimetallic nanoparticles (Rosbero *et.al,* 2016). In DLS, light from a coherent source is directed at a particle suspension where it is scattered (Filella *et al.,* 1997 and Schurtenberger *et al.,* 1993). Due to the random Brownian motion of the particles, the scattering fluctuates with time due to the constantly changing distances of the scatterers. Hence the size of ionic liquid and plant extract mediated nanoparticles, determined by DLS, may appear smaller than plant mediated nanoparticle without ionic liquid when palladium is considered. Plant-mediated nanoparticles are in most studies fast aggregating. DLS in this work is recorded after four hours of ageing. DLS has previously been used to determine the size distribution profile of nanoparticles in suspension (Saxena *et al.,* 2010 and Francois *et al.,* 2020).

Thermogravimetric and Differential Thermal Analysis (TGDTA)

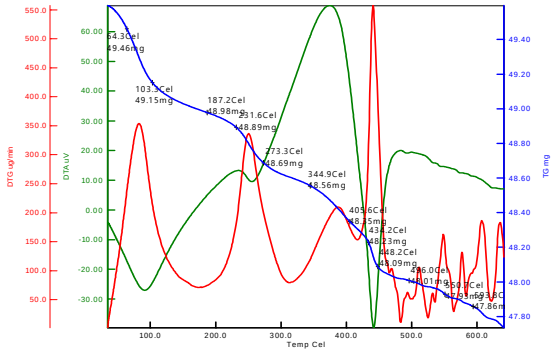

Fig. 8. TGDTA image of Cu-Ag NPs.

The TG analysis of Cu-Ag NPs synthesized by using *Tabernaemontana divaricata* is represented in Fig. 8. The temperature range is 50^{0} C to 700^{0} C. The initial weight loss observed at 54^{0} C corresponds to that of loss of nitrates compounds. The peak observed after 230^{0} C corresponds to decomposition of covalently bond organic material, mainly nitrate which was converted into oxide at the time of synthesis. From DTA curves of Cu-Ag NPs the exothermic peak present in between 250^{0} C to 550 °C can be observed due to desorption and decomposition of nitrate compounds. In TG analysis, the initial weight loss observed is below the 54^{0} C, it shows that the loss of water which is evaporated on the surface of the sample. Beyond this temperature the peak increment is because of adsorption due to the decomposition of covalently bound organic material (Ruparelia *et al.,* 2008; Tamayo *et al.,* 2014). The weight loss of the Cu-Ag NPs synthesized is calculated to be 20.5%.

Fluorescence spectroscopy analysis

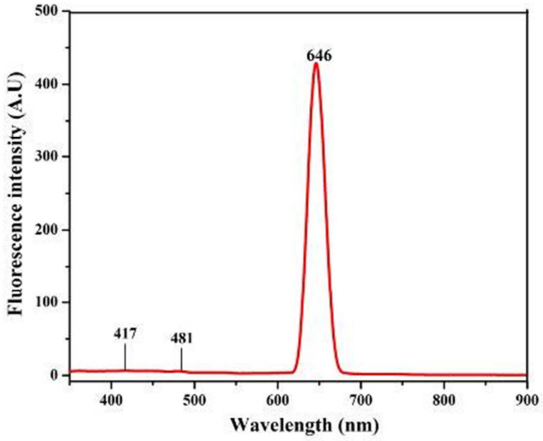

Fig. 9. Fluorescence spectrum of Cu-Ag NPs.

Fluorescence spectra of Cu-Ag NPs were recorded at room temperature by Fluorescence spectrophoto meter as shown in Fig. 9. Measurements were made over the wavelength range of 300-900nm. Intensities of maximum wavelength emissions were collected from the experiments as shown in Fig. 9 and the emission values were plotted as wavelength (nm) vs Intensity (A.U). As reported previously, the rotation speed of the rotating electrode has a significant effect on the particle size and degree of aggregation, and at higher rotational speed, the synthesis of smaller nanoparticles is favorable. We also observed that

Enhancement in the rotation speed of the rotating electrode is accompanied by a decrease in the size of the prepared Ag NPs (Ma *et al.,* 2004 and Paranga *et al.,* 2012). Fig. 8 shows three characteristic peaks of Cu-Ag NPs. The lower emission peak was attributed at 417nm representing the Cu-Ag NPs formation and a higher emission peak was measured with an excitation wavelength of 646nm may attribute to the surface defects.

The fluorescence spectra were the most preferable technique for investigating energy levels. An increase in fluorescence intensity with increasing Cu-Ag NPs size was observed.

Antibacterial Activity

Antibacterial activity of incorporated Cu-Ag NPs was performed by agar well diffusion method against *Staphylococcus aureus, Bacillus subtilis, Enterobactersp, Pseudomonas auroginosa,* and *E. coli* (Fig. 10). Pathogenic bacteria are grown in nutrient broth and 24 h culture of these strains were swabbed uniformly onto the individual's plates containing Muller hinton agar using sterile cotton swabs. About 5 wells were made and the purified Cu-Ag NPs at different weight like 25µl, 50µl, 75µl and 100µl were added into each well on all plates. The plates were incubated for 24 h at 37°C in an incubator. After incubation the different levels of zone formation around the well was measured. Also the zone of inhibition of Cu nanoparticles is somewhat larger than Ag nanoparticles. In case of bimetallic systems, the zone of inhibition increases with increasing Cu concentrations which again supports the efficiency of Cu nanoparticles.

The results indicated that the metallic nanoparticles exhibited excellent antibacterial activity against bacteria even at concentrations as low as 0.3mg/L. Therefore, it could be concluded that silver and copper ions could be released through aqueous starch solutions owing to the stable dispersion at molecular level in the solution. The slow diffusion of metal ions from the stabilizing medium is responsible for the antibacterial activity. It may be reasonably presumed that such a composite of metallic nanoparticles with biopolymers will benefit prolonging the release time of Ag particles and preserving the sustained antibacterial behaviour. The results in Table 1 also indicate that the nanoparticles are more effective against E. coli than S. aureus. (Kim *et al.*, 2007; Mayur Valodkar *et al.*, 2011) reported greater biocidal efficiency of silver nanoparticles for E. coli, and attributed it to difference in cell wall structure between gram negative and gram positive microorganisms. Among the two metals, copper was observed to be more efficient than silver unlike reported (Ruparelia *et al.*, 2008, Mayur Valodkar *et al.*, 2011), who attributed lower activity of copper nanoparticles to the oxide layer present on the surface.

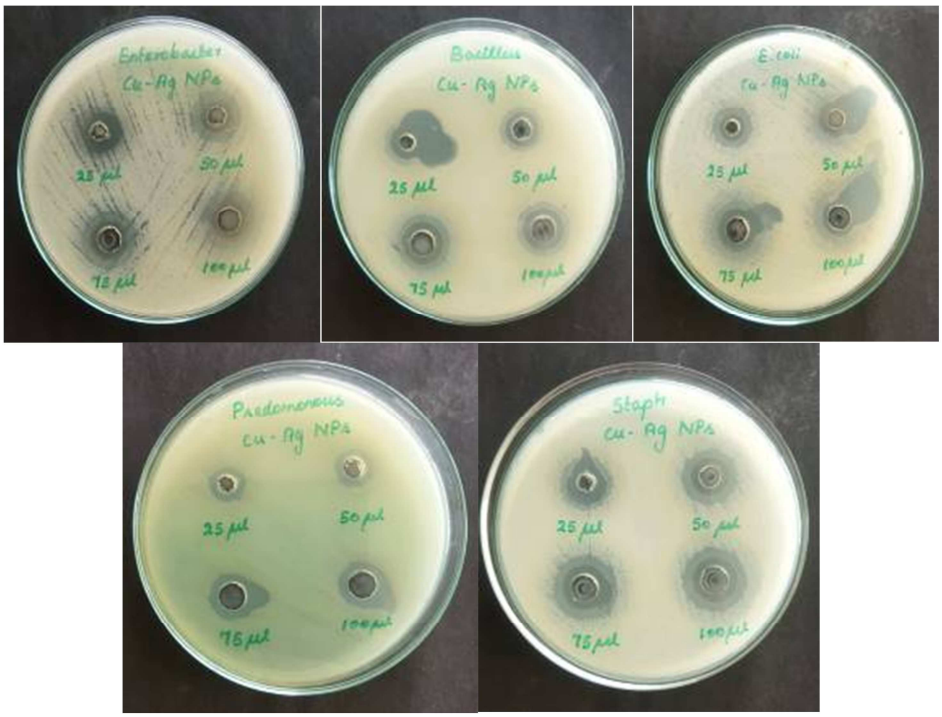

Fig. 10. Zone of inhibition of Cu-Ag NPs against various bacterial strains.

Table 2. Zone of inhibition of Cu-Ag bimetallic NPs against selected bacterial Strains.

Concentration	Zone of Inhibition (mm in diameter)				
	Bacillus sp	E. coli	Enterobacter sp	Staphylococcus aureus	Pseudomonas sp
25µl	1.2	1.2	1.6	1.5	1.1
50µl	1.2	1.4	1.7	1.7	1.2
75µl	1.4	1.7	2.0	1.9	1.4
100µl	1.6	1.9	2.1	2.0	1.6

Conclusion

This work highlights the green synthesis of bimetallic Cu-Ag NPs using *Tabernaemontana divaricata* leaf extract. The novelty of this work was the usage of *Tabernaemontana divaricata* leaves extract as capping reagent to reduce the average bimetallic particle size to 60nm. Various structural and morphological characterizations of the as-prepared nanoparticles through particle size analyzer, SEM, EDX, and XRD showed the complete synthesis of copper-silver nanoparticles with a very low amount of their respective oxides.

Application studies for the as-prepared bimetallic nanoparticles exhibited an excellent antibacterial ability to show that the zone of inhibition was almost similar for both gram-positive and gram-negative bacteria. Thus, a cost-effective, non-toxic, and green technique to produce high-quality copper-silver bimetallic nanoparticle system is reported. A detailed study on the industrial and commercial application of the prepared bimetallic nanoparticles can be carried out as future scope of the present work.

Reference

Chaloupka K, Malam, Seifalian AM. 2010. Nano silver as a New Generation of Nano product in Biomedical Applications. Trends Biotechnology **28,** 580-586

Chattopadhyay DP, Patel BH. 2009. Improvement in physical and dyeing properties of natural fibres through pre-treatment with silver nanoparticles. Indian Journal of Fibre and Textile Research **34(4),** 368-373.

Cioffi N, Torsi L, Ditaranto N, Tantillo G, Ghibelli L, Sabbatini L, Bleve-Zacheo T, D'Alessio M, Zambonin PG, Traversa E. 2005. Copper Nanoparticle/Polymer Composites with Antifungal and Bacteriostatic Properties. Chem. Mater **17,** 5255-5235.

Dang TMD, Le TTT, Fribourg-Blanc E, Dang MC. 2011. The influence of solvents and surfactants on the preparation of copper nanoparticles by a chemical reduction method. Adv. Nat. Sci. Nanosci. Nanotechnol **2,** 025004-025007.

Deepika Sharma, Lalita Ledwani, Naveen Kumar, Tarang Mehrotra, Naveed Pervaiz, Ravinder Kuma. 2020. An Investigation of Physicochemical and Biological Properties of Rheum emodi Mediated Bimetallic Ag-Cu Nanoparticles. Arabian Journal for Science and Engineering **46,** 1-11.

Filella M, Zhang J, Newman ME, Buffle J. 1997. Analytical applications of photon correlation spectroscopy for size distribution measurements of natural colloidal suspensions: capabilities and limitations. Colloids Surf A **120,** 27-46.

Francois, Agnes Ntoumba, Philippe Belle Kedi, Edmond choumbi, Alexa Schmitz, Laura Schmolke, Maximilian Klopotowski, Bastian Moll, Ülkü Kökcam-Demir, Emmanuel Albert Mpondo, Leopold Gustave Lehman, Christoph Janiak. 2018. Silver and palladium nanoparticles produced using a plant extract as reducing agent, stabilized with an ionic liquid: sizing by X-ray powder diffraction and dynamic light scattering. Journal of materials research and technology **8(2),** 1991-2000

Gupta AS, Mumtaz CH, Li I, Hussain, Rotello VMJCSR. 2019. Combatting antibiotic-resistant bacteria using nanomaterials. Chemical society reviews **48(2),** 415-427.

Hikmah NNF, Idrus J, Jai AH. 2016. Synthesis and characterization of silver-copper core-shell nanoparticles using polyol method for antimicrobial agent. International Conference on Chemical Engineering and Bioprocess Engineering, IOP Conf. Series: Earth and Environmental Science **36,** 37-39.

Ikram M, Khan MI, Raza A, Imran M, Ul-Hamid A, Ali S. 2020. Outstanding performance of silver decorated MoS2 nano petals used as nanocatalysts for synthetic dye degradation. Physica E: Low dimensional Systems and Nanostructures **4,** 124-126

Jeon HJ, Yi SC, Oh SG. 2003. Preparation and Antibacterial Effects of Ag-SiO2 Thin Films by Sol-Gel Method. Biomaterials **24,** 4921-4928.

Kim JS, Kuk E, Yu KN, Kim J, Park SJ, Lee, HJ, Kim SH, Park YK, Park YH, Hwang CY, Kim, YK, Lee Y, Jeong, D, Cho MH. 2007. Antimicrobial effects of silver nanoparticles. Nanomed-Nanotechnol **3,** 95-101.

Klabunde K, Richards R. *2001*. Nanoscale materials in chemistry. (Hoboken, New Jersey: Biblioteca eon línea de Wiley) 1035-1037.

LimL, Nan D, Xu G, Rend KY. *2015*. Antibacterial performance of a Cu-bearing stainless steel against microorganisms in tap water. Journal of Materials Science and Technology **31(3),** 243-251.

Liu JF, Li C, Liu. 2014. Effect of Cu content on the antibacterial activity of titanium-copper sintered alloys. Materials Science and Engineering C **35(1),** 392-400.

Liu Y, Wei S, Gao W. 2015. Ag/ZnO heterostructures and their photocatalytic activity under visible light: effect of reducing medium. J. Hazard. Mater **287,** 59-68.

Liz-Marzan LM. 2004. Nanometals: formation and color Mater. Today **7,** 26-31.

Ma H, Yin B, Wang S, Jiao Y, Pan W, Huang S, Chen S, Meng F. 2004. Synthesis of silver and gold nanoparticles by a novel electrochemical method, Chem. Phys. Chem **5,** 68-75.

Ma ZD, Kim, AT, Adesogan SK, Galvao K, Jeong KC. 2016. Chitosan Microparticles Exert Broad- Spectrum Antimicrobial Activity against Antibiotic-Resistant Micro-organisms without Increasing Resistance. ACS Applied Materials and Interfaces **8(17),** 10700-10709.

Mayur Valodkar, Shefaly Modi, Angshuman Pal, Sonal Thakore. 2011. Synthesis and anti-bacterial activity of Cu, Ag and Cu-Ag alloy nanoparticles: A green approach. Materials Research Bulletin **46,** 384-389

Niu, JY Sun, F Wang, C Zhao, J Ren, X Qu. 2018. Photomodulated Nanozyme Used for a Gram-Selective Antimicrobial. Chemistry of Materials **30(20),** 7027-7033.

Pal S, Yoon EJ, Tak YK, Choi EC, Song JM. 2009. Synthesis of Highly Antibacterial Nanocrystalline Trivalent Silver Polydiguanide. J. Am. Chem. Soc **131,** 16147.

Paranga Z, Keshavarzb A, Farahi S, Elahi SM, Ghorannevissa M, Parhoodeh S. 2012. Fluorescence emission spectra of silver and silver/cobalt nanoparticles. Scientia Iranica F **19 (3),** 943-947.

Rahman A, Ismail A, Jumbianti D, Magdalena S, Sudrajat H. 2009. Synthesis of copper oxide nanoparticles by using *Phormidium cyanobacterium*, Indonesian Journal of Chemistry **9,** 355-360.

Ruparelia JP, Chatterjee AK, Duttagupta SP, Mukherji S. 2008. Strain specificity in antimicrobial activity of silver and copper nanoparticles. Acta Biomater **4,** 707-716.

Ruparelia JPAK, Chatterjee, Duttagupta SP, Mukherji S. 2008. Strain specificity in antimicrobial activity of silver and copper nanoparticles. Acta Biomaterialia **4(3),** 707-716.

Saxena A, Tripathi RM, Singh RP. 2010. Biological synthesis of silver nanoparticles by using onion (*Allium cepa*) extract and their antibacterial activity. Digest J Nanomater Biostr **5,** 427-32.

Schurtenberger P, Newman ME. 1993. Characterization of biological and environmental particles using static and dynamic light scattering. Taylor and Francis, Environmental particles 1st edition **2,** 79.

Shankar SS, Ahmad A, Sastry M. 2003. Geranium leaf assisted biosynthesis of silver nanoparticles. Biotechnol. Prog **19,** 1627-1631.

Sonal T, Padamanabhi S, Nagar R, Jadeja N, Menaka T, Ranjitsinh V, Devkar P, Singh R. 2019. Sapota fruit latex mediated synthesis of Ag, Cu mono and bimetallic nanoparticles and their in vitro toxicity studies. Arabian Journal of chemistry **12,** 694-700.

Sondi I, Salopek-Sondi B. 2004. Silver Nanoparticles as Antimicrobial Agent: a Case Study on E. coli as a B Model for Gram-Negative Bacteria. J. Colloid Interface Sci **275,** 177.

Sun Y, Xia Y. 2002. Shape-controlled synthesis of gold and silver nanoparticles. Science **298,** 2176-2179.

Tamayo, Zapata LAPA, Vejar ND. 2014. Release of silver and copper nanoparticles from polyethylene nanocomposites and their penetration into *Listeria monocytogenes*, Materials Science and Engineering *C* **40,** 24-31.

Tan KS, Cheong KY. 2013. Advances of Ag, Cu, and Ag-Cu alloy nanoparticles synthesized via chemical reduction route. J. Nanopart. Res **15,** 1-29.

Tang XF, Yang ZG, Wang WJ. 2010. A simple way of preparing high-concentration and high-purity nano copper colloid for conductive ink in inkjet printing technology. Colloids Surf. A **360,** 99-104.

Therese Marie SR. Drexel HC. 2016. Green preparation and characterization of tentacle-like silver/copper nanoparticles for catalytic degradation of toxic chlorpyrifos in water. Journal of Environmental Chemical Engineering **9(4).**

Valodkar M, Modi S, Pal A, Thakore S. 2011. Synthesis and anti-bacterial activity of Cu, Ag and Cu-Ag alloy nanoparticles: a green approach. Mater. Res. Bull **46,** 384-389.

Xiu Zm, Zhang Qb, Puppala HL, Colvin VL, Alvarez PJJ. 2012. Negligible Particle-Specific Antibacterial Activity of Silver Nanoparticles. Nano Lett **12,** 4271.

Yin M, Wu CK, Lou Y. 2005. Copper oxide nanocrystals, Journal of the American Chemical Society **127(26),** 9506-9511.

Zhao X, Wang L, Tang C, Zha X, Yong L, Su B, Kai K, Rui-Ying B, Yang M, Wei Y. 2020. Smart Ti3C2Tx MXene Fabric with Fast Humidity Response and Joule Heating for Healthcare and Medical Therapy Applications. ACS Nano **14 (7),** 8793-8805.